Research Article

Mathematical modeling of bioethanol production from sweet sorghum juice under high gravity fermentation: Applicability of Monod-based, logistic, modified Gompertz and Weibull models
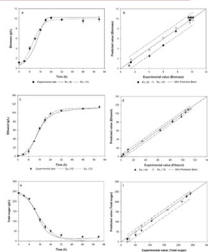
Apilak Salakkam [a,b], Niphaphat Phukoetphim [a], Pattana Laopaiboon [a,b], Lakkana Laopaiboon [a,c,*]

[a] *Department of Biotechnology, Faculty of Technology, Khon Kaen University, Khon Kaen 40002, Thailand*
[b] *Fermentation Research Center for Value Added Agricultural Products, Khon Kaen University, Khon Kaen 40002, Thailand*
[c] *Center for Alternative Energy Research and Development, Khon Kaen University, Khon Kaen 40002, Thailand*

GRAPHICAL ABSTRACT

ARTICLE INFO

ABSTRACT

Background: Mathematical modeling of a fermentation process is crucial in understanding and predicting dynamics of the process, which can be used in process improvement, design and control. The present study aimed to develop Monod-based kinetic models to describe cell growth, substrate consumption and ethanol production by *Saccharomyces cerevisiae* NP 01 under high gravity (HG) fermentation of sweet sorghum juice (SSJ).
Results: The fermentation using an initial total sugar (TS) concentration of 240 g/L resulted in 113.3 g/L of ethanol production, with 90.9% TS consumption and a fermentation efficiency of 94.4%. Growth of the yeast in terms of specific growth rate was found to be inhibited at a threshold TS concentration of 65 g/L, and the maximum specific growth rate, Monod constant and inhibition constant were 0.45 1/h, 19.5 g/L and 0.002 L/ (g·h), respectively. Monod-based models incorporating substrate and product inhibition terms showed high applicability to describe the changes of cell, TS and ethanol concentrations, based on the values of bias factor, accuracy factor, coefficient of determination and root mean square error.
Conclusions: The Monod-based models fitted the data equally well as compared with the logistic, modified Gompertz, and Weibull models, despite estimating the value of different kinetic parameters. These results demonstrated that all the models tested were applicable in modeling HG ethanol fermentation.

Nomenclature

e	Euler's number (2.71828)
i	Inhibition constant (L/(g·h))
K_S	Monod constant (g/L)
K_{SP}	Saturation constant for product formation (g/L)
L	Lag time (h)
n	number of observations
P	Product concentration (g/L)
P_0	Initial product concentration (g/L)
P_m	Maximum product concentration (g/L)
$P_{X,m}$	Production concentration that causes growth inhibition (g/L)
q	Specific product formation rate (1/h)
q_m	Maximum specific product formation rate (1/h)
R_m	Maximum rate of production formation (g/(L·h))
S	Substrate concentration (g/L)
S^*	Threshold substrate concentration (g/L)
t	time (h)
TS	Total sugar concentration (g/L)

TS_{Ini}	Initial total sugar concentration (g/L)
x_i	Experimental data at time i
X	Biomass concentration (g/L)
X_0	Initial biomass concentration (g/L)
X_m	Maximum biomass concentration (g/L)
y_i	Predicted data at time i
$Y_{P/S}$	Product yield on substrate (g/g)
$Y_{X/S}$	Biomass yield on substrate (g/g)

Greek letters

α	Scale parameter used to indicate how fast substrate is consumed
β	Shape parameter determining the direction of the concavity of the curve
μ	Specific growth rate (1/h)
μ_m	Maximum specific growth rate (1/h)

---

1. Introduction

Bioethanol is one of the most widely used biofuels in modern society, owing to its renewability and environmental friendliness [1]. It is typically used in the form of gasohol after blending with gasoline at different proportions, i.e., 5% to 85% by volume [2]. According to the outlook by the Organization for Economic Co-operation and Development (OECD) and the Food and Agriculture Organization of the United Nations (FAO), the global consumption of ethanol fuel was over 117 billion liters in 2020, and this will be increasing to over 132 billion liters in 2030, with the majority of ethanol (*ca.* 88%) being produced from corn and sugarcane [3]. This large and increasing consumption of first-generation (1G) ethanol would inevitably lead to the competitive utilization of biomass for food and fuel productions [4], resulting in competition with food security [5]. This problem is believed to be mitigable by using second-generation (2G) ethanol that is produced from inedible biomass, e.g., lignocellulosic materials and wasted starch-rich biomass [1,6,7,8,9,10]. However, low saccharification efficiency and ethanol yield, as well as the use of cost-intensive processing technology, are still the major hurdles impeding the large-scale production of 2G ethanol [11,12].

Besides the carbohydrate-rich biomasses, other high-potential ethanol feedstocks are those that are sugar-rich, e.g., sweet sorghum juice (SSJ). Sweet sorghum (*Sorghum bicolor* L. Moench) is a C4 plant that can be cultivated in temperate regions. Aside from its short production cycle, this plant has advantages of being resistant to drought, salinity and flooding [13,14], and has lower requirement of fertilizer and water as compared with sugarcane and corn [14,15]. Juice of sweet sorghum also has similar composition to sugarcane juice [15] as it contains sucrose, glucose and fructose as the major components [14], making it readily usable in the existing sugarcane ethanol production facility. However, comparing with the use of sugarcane juice, fermentation of fresh SSJ tends to result in lower ethanol titer as SSJ has lower sugar yield [15]. In this regard, SSJ can be concentrated and fermented under high gravity (HG: 180–240 g/L of sugars) or very high gravity (VHG: $\geq$ 250 g/L of sugars) conditions to achieve higher ethanol content [16,17]. This strategy has long been demonstrated to effectively improve ethanol yield [18], which consequently helps to reduce distillation costs [17]. However, in view of process performance and economics, VHG fermentation might not be practically feasible as the growth of the ethanol producer is usually inhibited by the high osmotic pressure, leading to prolonged fermentation time, low ethanol productivity, and incomplete substrate utilization [17,18]. These have been demonstrated experimentally in a study of Camargos et al. [17] and Laopaiboon et al. [19], where the growth of *Saccharomyces cerevisiae* and other ethanol producers were retarded in sugarcane molasses-based medium containing 250 g/L of sugar, and SSJ containing 280 g/L of sugar, respectively. Furthermore, although the use of VHG fermentation could save energy for ethanol distillation and stillage treatment [20], it might not be actually economically viable since the concentration of substrate was very energy intensive, and the advantage of energy saving in ethanol recovery step was not prominent [21]. The use of HG fermentation, on the other hand, encounters less problem of substrate inhibition and still gives satisfactory ethanol yield [19]. Therefore, it is considered a more suitable process for large-scale ethanol fermentation.

HG fermentation of SSJ has been widely investigated in the past decades. Literature survey revealed that most studies aimed mainly to improve the growth and osmotolerance of the ethanol producers to achieve higher ethanol titer. Process improvement by, for example, nutrients supplementation, e.g., yeast extract and dry spent yeast, and aeration have been investigated [16]. Fermentation conditions, e.g., inoculum size, initial sugar concentra-

tion, agitation rate and temperature, have been optimized [22,23], and different fermentation modes and strategies, e.g., fed-batch [17], repeated-batch [24], and continuous [25] fermentations, as well as cell immobilization [23], and microaeration [26], have been tested. However, less attention has been paid to process modeling despite this being important to understand the process dynamics and predict the process performance, which are essential in the improvement, design and control of the process [27]. Furthermore, most of the relevant studies reported either the development of Monod-based model [25,28] or the use of other unstructured models [29] to predict changes during the fermentation, and no direct comparisons on the applicability of these models have been reported, leaving a question as to which equation would be more suitable for process modeling. Therefore, with the advantages of HG fermentation, and the limited information on the applicability of Monod-based and other unstructured models on ethanol fermentation, the present study investigated the use of concentrated SSJ as the substrate for HG ethanol fermentation. Based on the results, Monod-based models were developed to predict the dynamics of cell growth, total sugar (TS) consumption, and ethanol production, and their applicability was compared with other unstructured models, i.e., logistic, modified Gompertz, and Weibull models, through the calculation of bias factor (*BF*), accuracy factor (*AF*), coefficient of determination (R^2), and root mean square error (*RMSE*).

2. Materials and methods

2.1. Microorganism and inoculum preparation

S. cerevisiae strain NP01 was used as the ethanol producer. It was isolated from a starter of Sato (Thai rice wine) and has been preserved in the Bioalcohol Fermentation Research Laboratory at the Faculty of Technology, Khon Kaen University, Thailand [16]. Inoculum was prepared by growing the yeast in 100 mL of yeast extract and malt extract (YM) medium comprising 3 g/L of yeast extract, 3 g/L of malt extract, 5 g/L of peptone and 10 g/L of glucose, at 30°C, 200 rpm for 18 h. After that, the culture (10%, v/v) was transferred to 350 mL of SSJ containing 100 g/L of TS and further incubated under the same conditions for 15 h. The active yeast cells were then harvested by centrifugation at 8,000 rpm for 10 min before used as the inoculum.

2.2. Preparation of sweet sorghum juice and ethanol production medium

Stalks of sweet sorghum *cv.* KKU40 were provided by the Division of Agronomy, Faculty of Agriculture, Khon Kaen University, Thailand. These were milled using a sugarcane juice extractor to obtain sweet sorghum juice (SSJ), which contained *ca.* 51 g/L of glucose, 43 g/L of fructose, and 61 g/L of sucrose [30]. SSJ was subsequently concentrated by heating to increase the soluble solid content from 16.6 to *ca.* 65°Brix. The concentrated SSJ was stored in plastic bags at −20°C until use. Ethanol production medium was prepared by diluting the concentrated SSJ with distilled water to 240 g/L of total sugar (TS), and supplementing with 9 g/L of yeast extract without pH adjustment [29]. Initial pH of the ethanol production medium was 4.54.

2.3. Ethanol fermentation

Five-hundred mL Erlenmeyer flask containing 350 mL of ethanol production medium was closed with an airlock and autoclaved at 110°C for 28 min [24]. After that, *S. cerevisiae* NP 01 was inoculated into the ethanol production medium to obtain an initial cell concentration at *ca.* 5×10^7 cells/mL. The fermentation was carried out at 30°C and agitation rate of 100 rpm for 60 h. Samples were taken at time intervals for the determinations of biomass growth, sugar consumption, and ethanol production. The sample was centrifuged at 13,000 rpm for 10 min, and the cell pellet was used for cell dry mass (CDM) determination, whereas the supernatant was used for TS and ethanol analyses. This experiment was conducted in triplicate, and the mean and standard deviation of the mean are reported.

2.4. Analytical methods

CDM was determined gravimetrically after washing the cells twice with distilled water and drying at 90°C until a constant weight was reached. Concentration of TS was determined using a phenol sulfuric acid method [31] using glucose (AR grade) as the standard. Ethanol concentration was determined using gas chromatography using 2-propanol as the internal standard [24]. Yields of biomass ($Y_{X/S}$) and ethanol ($Y_{P/S}$) on TS were calculated using Equation 1 and Equation 2, respectively, where X_{Fin} is the final CDM concentration (g/L), X_{Ini} is the initial CDM concentration (g/L), TS_{Ini} is the initial TS concentration (g/L), TS_{Fin} is the final TS concentration (g/L), and *EtOH* is the ethanol concentration (g/L). Equation 3 was used to calculate the fermentation efficiency, where $Y_{P/S,Th}$ is the theoretical yield of ethanol obtained from a stoichiometric conversion of sucrose to ethanol (0.54 g/g).

$$Y_{X/S} = \frac{X_{Fin} - X_{Ini}}{TS_{Ini} - TS_{Fin}} \qquad \text{Equation 1}$$

$$Y_{P/S} = \frac{EtOH}{TS_{Ini} - TS_{Fin}} \qquad \text{Equation 2}$$

$$Eff_{Ferm} = \frac{Y_{P/S}}{Y_{P/S,Th}} \times 100 \qquad \text{Equation 3}$$

2.5. Modeling of yeast growth, substrate consumption and ethanol production

2.5.1. Estimation of maximum specific growth rate and Monod constant

Concentrated SSJ was diluted with distilled water to contain 40 to 220 g/L of TS, supplemented with 9 g/L of yeast extract, and autoclaved at 110°C for 28 min. After that, inoculum of *S. cerevisiae* NP01 was transferred to the juice at 10% (v/v), and the cultures were incubated at 30°C, 100 rpm for 24 h. Samples were collected at time intervals and used for CDM measurement. For each TS concentration, CDM concentrations were plotted against time in a log-linear scale, and specific growth rate (μ) of the yeast was estimated as the largest slope of the plot, which represented the exponential phase of the yeast growth [32]. To obtain the value of maximum specific growth rate (μ_m) and Monod constant (K_S), a plot between μ and TS concentration was fitted with a substrate inhibition model proposed by Tseng and Wayman [33] [Equation 4]. The inhibition constant (*i*) in Equation 4 represents the severity of inhibition caused by the substrate, and S^* is the threshold TS concentration (g/L), beyond which inhibition of growth is observed.

$$\mu = \frac{\mu_m S}{K_S + S} - i(S - S^*) \qquad \text{Equation 4}$$

2.5.2. Mathematical modeling

For batch fermentation without substrate and product inhibitions, dynamics of cell growth and ethanol production can be described using Equation 5 and Equation 6, respectively. In the

absence of inhibitors, μ and q obey Monod kinetics [Equation 7 and Equation 8, respectively].

$$\frac{dX}{dt} = \mu X \qquad \text{Equation 5}$$

$$\frac{dP}{dt} = qX \qquad \text{Equation 6}$$

$$\mu = \frac{\mu_{\mathrm{m}}S}{K_S + S} \qquad \text{Equation 7}$$

$$q = \frac{q_{\mathrm{m}}S}{K_{SP} + S} \qquad \text{Equation 8}$$

However, during a HG fermentation, the high concentrations of sugar and ethanol can be the inhibitory factors hampering the activity of the cells [25]. For this reason, Equation 5 and Equation 6 were modified by incorporating terms representing the substrate and product inhibitions. Considering that both high substrate concentration and the presence of ethanol could be inhibitory to cell growth, terms for substrate inhibition [33] and product inhibition [34] were added to Equation 7, and the resulting equation was substituted to Equation 5, yielding Equation 9 for describing cell growth during the fermentation. On the other hand, for ethanol production, a product

inhibition [34] term was added to Equation 8, and the resulting equation was substituted to Equation 6, yielding Equation 10. As for substrate consumption, since sugar is mainly consumed for cell growth, cell maintenance, and ethanol production [28], the rate of substrate consumption can be described by Equation 11, where m is the maintenance coefficient (1/h).

$$\frac{dX}{dt} = \left[\left(\frac{\mu_{\mathrm{m}}S}{K_S + S} - i(S - S^*) \right) \left(1 - \frac{P}{P_{X,\mathrm{m}}} \right) \right](X) \qquad \text{Equation 9}$$

$$\frac{dP}{dt} = \left[\left(\frac{q_{\mathrm{m}}S}{K_{SP} + S} \right) \left(1 - \frac{P}{P_{\mathrm{m}}} \right) \right](X) \qquad \text{Equation 10}$$

$$-\frac{dS}{dt} = \frac{1}{Y_{X/S}} \left(\frac{dX}{dt} \right) + \frac{1}{Y_{P/S}} \left(\frac{dP}{dt} \right) + mX \qquad \text{Equation 11}$$

To compare the applicability of the Monod-based models [Equation 9, Equation 10, Equation 11], based on our previous study [29], logistic [Equation 12] and modified Gompertz [Equation 13] models were used to fit the cell growth and ethanol production, respectively. As for the substrate consumption, Weibull distribution [Equation 14] was used to fit the TS profile [35]. The value of α in Equation 14 indicated the rate of TS consumption, i.e., the smaller α indicated rapid TS consumption. The value of β
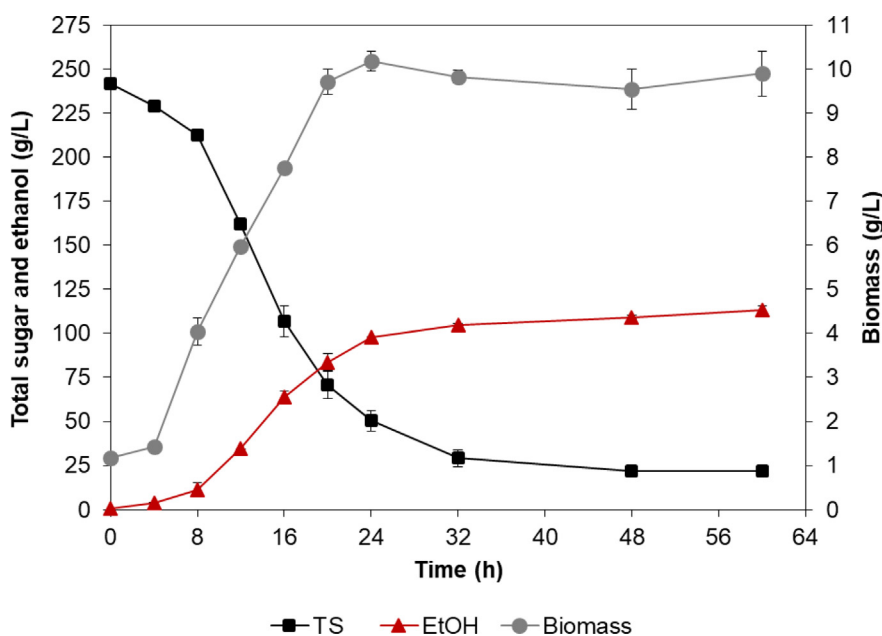
Fig. 1. Growth, total sugar consumption and ethanol production by *S. cerevisiae* NP01 growing on sweet sorghum juice containing 240 g/L of total sugar.

Table 1
Ethanol production from sweet sorghum juice under high gravity conditions.

Microorganism	Sugar concentration (g/L)	Sugar consumption (g/L)	Ethanol production (g/L)	Ethanol yield (g/g)	Fermentation efficiency (%)	Reference
S. cerevisiae SEMF1	185	180	86.2	0.48	88.9[a]	[38]
S. cerevisiae NRRL Y-2034	200	-	70.6	-	87.35	[22]
Yeast strain CAT-1	226	-	97.8	-	87.0[b]	[21]
Industrial strain (PAN)	237	213.3	103.7[c]	0.50	92.6[a]	[14]
S. cerevisiae KKU-VN8	200	-	89.32	-	96.32	[39]
S. cerevisiae SSJ01KKU	240	229.9	118.12	0.51	94.4[a]	[19]
S. cerevisiae NP01	241.5	219.5	113.3	0.51	94.4[a]	This study

[a] Calculated using Equation 3.
[b] Calculated based on an ethanol yield of 0.511 g-ethanol/g-glucose as reported in the original paper.
[c] Calculated from ethanol productivity and fermentation time reported in the original paper.
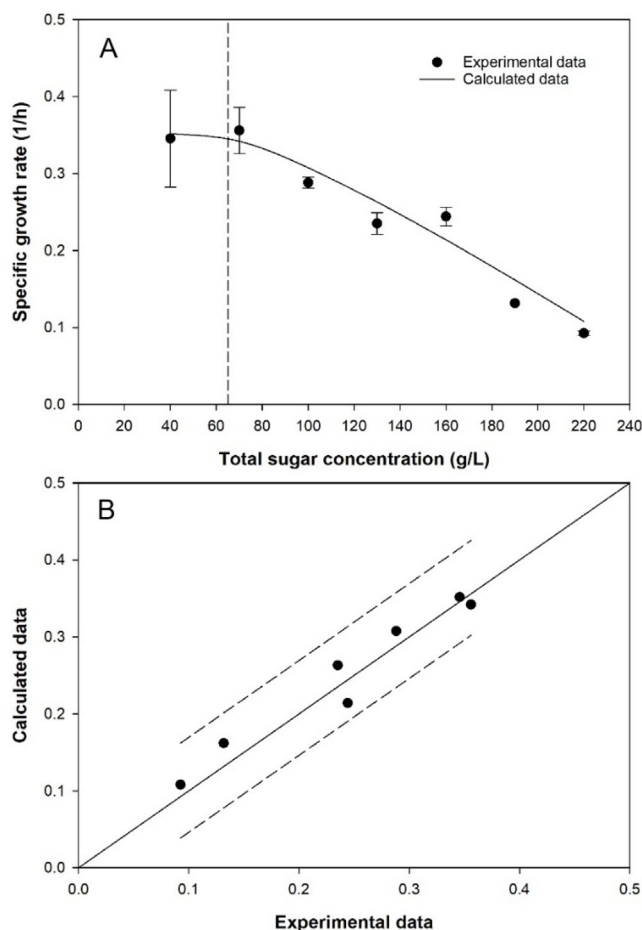
Fig. 2. Specific growth rate of *S. cerevisiae* NP01 growing on sweet sorghum juice containing 40 to 220 g/L (A), and correlation between the calculated and experimental data (B). The dashed line in (A) represents the threshold concentration of total sugar (65 g/L). The solid line in (B) represents a correlation coefficient of 1, and the dashed lines in (B) represent 95% prediction band.

determines the direction of the concavity, i.e., the curve is concave upward if $\beta < 1$, concave downward if $\beta > 1$, and linear if $\beta = 1$. Solver function of Microsoft Excel 2019 was used for curve fitting by minimizing the residual sum of square value. For the modeling using the Monod-based models, the Euler's method was used.

$$X = \frac{X_0 \exp(\mu_m t)}{1 - \left[\left(\frac{X_0}{X_m}\right)(1 - \exp(\mu_m t))\right]}$$

Equation 12

$$P = P_0 + \left[P_m \times \exp\left(-\exp\left(\frac{R_m e}{P_m}(L - t)\right) + 1\right)\right]$$

Equation 13

$$\log\left(\frac{TS}{TS_{Ini}}\right) = -\frac{1}{2.303}\left(\frac{t}{\alpha}\right)^{\beta}$$

Equation 14

2.5.3. Validation of the models

Bias factor (*BF*), which is a multiplicative factor by which a model overestimates or underestimates the data, and accuracy factor (*AF*), which is a measurement of the mean difference between the observed and predicted data, were used to validate the models. Ideally, the values of *BF* and *AF* are 1, which indicate no deviations between the observed and predicted data. *BF* and *AF* were calculated using Equation 15 and Equation 16, respectively [36]. Following the assumption given by Germec et al. [37], the model was considered "good" if $0.95 \leq BF \leq 1.11$, it was "acceptable" if

$0.87 \leq BF \leq 0.95$, or $1.11 \leq BF \leq 1.43$; and it was "unacceptable" if $BF < 0.87$ or $BF > 1.43$. On the other hand, if $1.00 \leq AF < 1.20$, the model is "good"; if $1.20 \leq AF \leq 1.30$, the model is "acceptable"' and if $AF > 1.30$, the model is "unacceptable". Fitting accuracy of the models was assessed using the coefficient of determination (R^2), which was obtained through a plot between the predicted and experimental values, the root mean square error (*RMSE*) [Equation 17], and the calculation of 95% prediction intervals using SigmaPlot version 14.

$$BF = 10^{\left(\sum \log(y_i/x_i)/n\right)}$$

Equation 15

$$AF = 10^{\left(\sum |\log(y_i/x_i)|/n\right)}$$

Equation 16

$$RMSE = \sqrt{\frac{\sum(x_i - y_i)^2}{n}}$$

Equation 17

3. Results and discussion

3.1. High gravity ethanol fermentation from SSJ by S. cerevisiae NP01

Fig. 1 shows that *S. cerevisiae* NP01 could grow well on SSJ containing 240 g/L of TS. pH of the medium decreased from 4.54 to 4.17 after 12 h. Then, the pH value slightly increased and the value was 4.35 at the end of fermentation. A log-linear plot of the biomass concentration against fermentation time (data not shown) revealed that the cells entered the exponential phase after the inoculation without observable lag phase. The exponential growth phase lasted until 20 h, and the cells entered the stationary phase afterward. The specific growth rate estimated during zero to 20 h was 0.115 1/h. The final cell concentration was 10.0 ± 0.5 g/L (*ca.* 2.5 to 2.7 × 10^8 cells/mL). Corresponding to the yeast growth, TS concentration dropped rapidly from 241.5 ± 1.3 to 50.5 ± 5.8 g/L during the first 24 h, and further decreased slowly to 22.0 ± 0.6 g/L at the end of the fermentation. Ethanol production was observed at as early as 6 h, and the concentration increased steadily to 98.0 ± 0.0 g/L at 24 h. Prolonging the process to 60 h resulted in a slight increase in ethanol concentration to 113.3 ± 2.3 g/L. Based on the initial (1.2 g/L) and maximum (10.2 g/L) biomass concentrations, TS consumption of 219.5 g/L (90.9% consumption), and the ethanol production of 113.3 g/L, $Y_{X/S}$ and $Y_{P/S}$ were calculated to be 0.04 g-biomass/g-TS, and 0.51 g-ethanol/g-TS, respectively. The fermentation efficiency of this process was 94.4%. Ethanol yield and fermentation efficiency obtained in this study were slightly higher than those reported by Zhao [38], Phutela and Kaur [22], Larnaudie et al. [21] and Rolz et al. [14], possibly due to the differences in yeast strains and fermentation conditions. Furthermore, it was found that ethanol production achieved in the present study was among the highest values reported in the literature using SSJ as the substrate (Table 1), indicating that *S. cerevisiae* NP01 was a highly efficient ethanol producer. Based on the results, it could be calculated that around 1.89 kg of TS (equivalent to 12.2 L and 12.7 kg of fresh SSJ, assuming that the density of SSJ containing 16°Brix was 1.04 g/mL [13]) would be required to produce 1 kg of ethanol (0.78 L of ethanol). This was equivalent to 61.42 L of ethanol per ton of fresh SSJ and 41.5 L per ton of sweet sorghum, assuming juice extraction ratio of 67.3% [13].

3.2. Estimation of μ_{max} and K_S for S. cerevisiae NP01 growing on SSJ

In microbial cultivation, the microbial growth rate can be related to the concentration of substrate through the Monod kinetics, which describes the change of μ as a function of a single limiting substrate concentration. According to the equation, μ increases
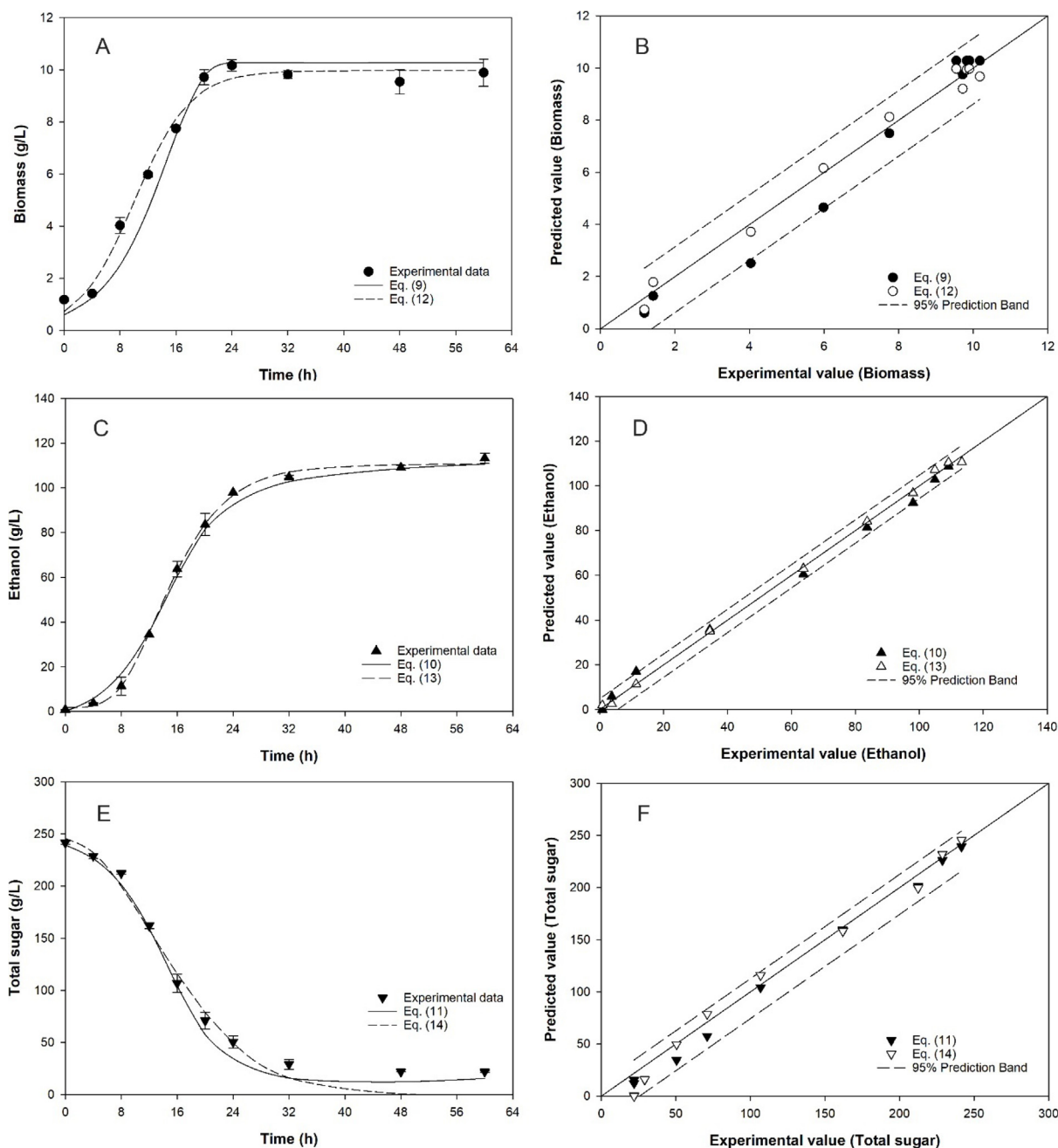
Fig. 3. Modeling of biomass growth (A and B), ethanol production (C and D) and total sugar consumption (E and F). Solid lines in (B), (D) and (F) represent a correlation coefficient of 1.

with increasing substrate concentration, approaching μ_m at high and saturating substrate concentration [40]. However, in some situations, e.g., under HG conditions, high substrate concentration could be inhibitory to microorganisms (μ decreases rather than approaching μ_m), and the Monod model inadequately describes this change. In the present study, the value of μ only increased, from 0.346 ± 0.063 to 0.356 ± 0.030 1/h, when TS concentration was increased from 40 to 70 g/L. Further increasing the TS concentration to 220 g/L resulted in a large drop of μ to 0.093 ± 0.003 1/ h (Fig. 2A). This suggested that inhibition of growth occurred at TS concentration beyond 70 g/L. The high concentration of fermentable sugars in the medium was thought to cause high osmotic pressure (hyperosmotic stress) that could affect the cell-cycle progression and cause changes in gene expression of the cells [41],

adversely affecting cell growth. Hyperosmotic stress could also cause changes in cellular physiology, e.g., budding manner, and retardation in cell division [42]. Decreases in cell viability were also reported as a result of changes in the cell membrane fluidity [43]. In the present study, the typical Monod model could not satisfactorily describe the change of μ, and therefore Equation 4 was used. The equation fitted the data well with R^2 of 0.9528 (Fig. 2A). The value of μ_m, K_S, and i was estimated to be 0.45 1/h, 19.5 g/L, and 0.002 L/(g·h), respectively. Based on curve fitting, the reduction of μ started at a threshold concentration (S^*) of 65 g/L. The degree of inhibition increased with increasing TS concentration since the difference between TS and the threshold concentrations ($S - S^*$) became larger. The model precited that the value of μ would be decreased linearly with increasing TS concen-

Table 2

Kinetic parameters estimated for biomass growth, total sugar consumption and ethanol production using Monod-based and other models. The values of bias factor, accuracy factor, R^2, and RMSE are also shown.

Monod-based models							
Equation 9 (cell growth)			Equation 10 (ethanol production)			Equation 11 (substrate consumption)	
μ_m	0.30		q_m	4.8		$Y_{X/S}$	0.44
K_S	21		K_{SP}	240		$Y_{P/S}$	0.53
i	0.00005		P_m	116.8		m	0.00
S^*	65						
$P_{m,x}$	86.9						
BF	0.87		BF	1.08		BF	0.95
AF	1.18		AF	1.11		AF	1.11
R^2	0.9789		R^2	0.9972		R^2	0.9978
RMSE	2.332		RMSE	9.764		RMSE	29.809
Logistic, modified Gompertz and Weibull models							
Equation 12 (cell growth)			Equation 13 (ethanol production)			Equation 14 (substrate consumption)	
X_0	0.7		P_0	1.8		TS_{Ini}	245.55
X_m	10.0		P_m	108.8		α	18.66
μ_m	0.25		R_m	7.2		β	1.86
			λ	7.4			
BF	0.97		BF	1.05		BF	0.36
AF	1.11		AF	1.14		AF	2.92
R^2	0.9888		R^2	0.9989		R^2	0.9882
RMSE	1.148		RMSE	4.421		RMSE	38.092

tration, and no growth (μ = 0 1/h) would be observed at *ca.* 280 g/L of TS. To validate the model, *BF* and *AF* were calculated, yielding the values of 1.06 and 1.11, respectively, indicating that the model had a good fit for the data set. The plot between the calculated and experimental data shows that the data points lie within the 95% prediction interval (Fig. 2B), confirming the accuracy of the model.

3.3. Modeling of biomass, ethanol and total sugar profiles

Data for biomass concentration were fitted using the Monod-based equation [Equation 9] and logistic model [Equation 12]. Equation 9 fitted the data well with R^2 of 0.9789, though it slightly underestimated the biomass concentration during the first 20 h. In terms of R^2, the logistic model gave a better fit, with the R^2 of 0.9888, due to the closer estimation of biomass growth during the first 20 h (Fig. 3A). *RMSE* value of Equation 12 was also lower than that of Equation 9 as seen in Table 2, confirming that the logistic model fitted the data better. Nevertheless, almost all the data estimated by both equations lied within the 95% prediction band (Fig. 3B), and the values of *BF* and *AF* for Equation 9 and Equation 12 were similar (Table 2) and were in the range of good fit. These implied that both models could well be used to predict the growth of the yeast. Based on the results given in Table 2, it can be seen that the Monod-based and logistic models estimated different kinetic parameters that were not interrelated [44]. For instance, Equation 9, which was developed based on Monod model, gave more details on the kinetics of cell growth, i.e., μ_m, K_S, i, S^*, and $P_{X,m}$, whereas Equation 12 gave only the values of X_0, X_m, and μ_m. The logistic model [Equation 12] did also not give information about the inhibition of growth that might have occurred as it does not have an inhibition term. Using Equation 9, it was possible to assess qualitatively the effects of substrate concentration and ethanol production on cell growth. For instance, the value of μ_m obtained in this experiment (0.30 1/h) was lower than that observed previously (0.45 1/h), while the value of K_S was slightly higher (21 against 19.5 g/L). Furthermore, the value of i was much lower in this experiment (5 $\times$ 10^{-5} against 0.002 L/(g·h)). This suggested that the ethanol present in the fermentation broth exerted inhibitory effects on growth of the yeast, and this effect

was stronger than that of high TS concentration (hyperosmotic pressure) alone. This was supported by Zhang [45] who reported that the end product or ethanol was the primary factor inhibiting yeast growth and fermentation activity. Cell growth and ethanol production were inhibited with the final product concentration, increasing only slightly with an increase in the initial substrate concentration. In our study, the $P_{X,m}$ value of 86.9 g/L was predicted to be the threshold concentration of ethanol, above which inhibition of growth occurred. Difference in $P_{X,m}$ value depends on yeast strain and fermentation processes [45,46].

Equation 10 and Equation 13 fitted the ethanol production data well with R^2 of 0.9972 and 0.9989, respectively (Fig. 3C). Despite the *RMSE* of Equation 13 was lower than that of Equation 10, all the data predicted by these models lied within the 95% prediction band (Fig. 3D), and *BF* and *AF* for both equations were very similar (Table 2) and were in the range of good fit. These suggested that the models could be used to describe the production of ethanol under the conditions tested. Again, although these models satisfactorily described the profile of ethanol, these predicted values of different parameters. Equation 10 predicted the value of maximum specific ethanol production rate (q_m) to be 4.8 1/h, with K_{SP} of 240 g/L. The maximum ethanol production was predicted to be 116.8 g/L, which was slightly higher than the experimental value (113.3 g/L). The values of q_m and P_m, and μ_m obtained using Equation 9, can be used in process control to, for instance, predict the time required to produce desired amount of product as demonstrated by Doran [47]. On the other hand, Equation 13 predicted that the maximum ethanol production was 108.8 g/L, slightly lower than the experimental value. However, it estimated the maximum ethanol production rate (R_m) to be 7.2 g/(L·h) and a lag time of 7.4 h. These values are useful for understanding, or better still, predicting the performance of the cells in response to the fermentation conditions. Furthermore, the rate of product formation and the final product concentration could be used in combination with mass balance equations to design and control the process [48].

Equation 11 and Equation 14 were used to fit the data for TS consumption. Both equations fitted the data well, with R^2 of 0.9848 and 0.9882, respectively. Equation 11 underestimated TS concentration after 20 h, and estimated $Y_{X/S}$ and $Y_{P/S}$ to be 0.49

and 0.50 g/g, respectively. The cell maintenance coefficient was estimated to be zero, which is typical as this is normally very low and could be negligible [25,49]. Inspection of the $Y_{X/S}$ and $Y_{P/S}$ revealed that $Y_{P/S}$ was very close to the experimental value (0.51 g/g), but $Y_{X/S}$ was around 12 times that of the experimental value. The overestimation of $Y_{X/S}$ was thought to be due to the consumption of TS to produce other metabolites, such as glycerol and organic acids (e.g., acetic, succinic, and pyruvic acids), that were not quantified in the present study [19]. Despite the discrepancy between the experimental and predicted values, the predicted $Y_{X/S}$ was similar to that reported in the literature, which ranged from 0.48 to 0.5 g/g [25,49]. As for Equation 14, it largely underestimated TS concentration after 32 h of the process and predicted a complete consumption of TS. The value of β was 1.86, indicating the downward concave curve of the TS profile. The large underestimation of TS concentration toward the end of the process using Equation 14 led to *BF* and *AF* of 0.36 and 2.92, respectively, which were outside the range of good fit. Furthermore, *RMSE* of Equation 14 was larger than that of Equation 11, i.e., 38.092 against 29.809. These indicated that Equation 11 was more suitable to fit the TS profile in the present study.

4. Conclusions

The present study investigated the production of ethanol from SSJ using *S. cerevisiae* NP01 under HG conditions. As high as 113. 3 ± 2.3 g-ethanol/L, with an ethanol yield of 0.51 g/g-TS and fermentation efficiency of 94.4%, was attained after 60 h of fermentation. Growth of the yeast, ethanol production and TS consumption could be described well using Monod-based kinetic models containing substrate and product inhibition terms. The use of logistic, modified Gompertz, and Weibull equations, were compared with the Monod-based models. Based on the calculation of *BF*, *AF*, R^2, and *RMSE*, it was found that all the models tested, except for the Weibull model, fitted the data well, and could well be used to describe or, better still, predict the performance of the process. However, since each model estimated the value of different kinetic parameters, it was considered that modeling of a fermentation process could be conducted using more than one model to obtain a more complete set of kinetic parameters for subsequent development and up-scaling of the process.

Author contributions

- Study conception and design: A Salakkam, P Laopaiboon, L Laopaiboon.
- Data collection: N Phukoetphim.
- Analysis and interpretation of results: A Salakkam.
- Draft manuscript preparation: A Salakkam.
- Revision of the results and approval of the final version of the manuscript: A Salakkam, P Laopaiboon, L Laopaiboon.

Financial support

Conflict of interest

None of the authors of this study has any financial interest or conflict with industries or parties.

References

[1] Khanpanuek S, Lunprom S, Reungsang A, et al. Repeated-batch simultaneous saccharification and fermentation of cassava pulp for ethanol production using amylases and *Saccharomyces cerevisiae* immobilized on bacterial cellulose. Biochem Eng J 2022;177:108258. https://doi.org/10.1016/j.bej.2021.108258.

[2] Suarez-Bertoa R, Zardini AA, Keuken H, et al. Impact of ethanol containing gasoline blends on emissions from a flex-fuel vehicle tested over the Worldwide Harmonized Light duty Test Cycle (WLTC). Fuel 2015;143:173–82. https://doi.org/10.1016/j.fuel.2014.10.076.

[3] Organisation for Economic Co-operation and Development: OECD-FAO. OECD-FAO Agricultural Outlook 2021-2030. [Internet]. July 2021 [cited 2022 Oct 10]. Available from: https://stats.oecd.org/.

[4] Prasad S, Ingle AP. Impacts of sustainable biofuels production from biomass. In: Rai M, Ingle AP, editors. Sustainable Bioenergy, vol. 12. Elsevier; 2019. p. 327–46. https://doi.org/10.1016/B978-0-12-817654-2.00012-5.

[5] Pachapur PK, Pachapur VL, Brar SK, et al. Food Security and Sustainability. In: Surampalli R, Zhang T, Goyal MK, editors. Sustainability: Fundamentals and Applications, vol. 17. p. 357–74. https://doi.org/10.1002/9781119434016.ch17.

[6] Devi A, Singh A, Bajar S, et al. Ethanol from lignocellulosic biomass: An in-depth analysis of pre-treatment methods, fermentation approaches and detoxification processes. J Environ Chem Eng 2021;9(5):105798. https://doi.org/10.1016/j.jece.2021.105798.

[7] Khonngam T, Salakkam A. Bioconversion of sugarcane bagasse and dry spent yeast to ethanol through a sequential process consisting of solid-state fermentation, hydrolysis, and submerged fermentation. Biochem Eng J 2019;150:107284. https://doi.org/10.1016/j.bej.2019.107284.

[8] Jin X, Song J, Liu GQ. Bioethanol production from rice straw through an enzymatic route mediated by enzymes developed in-house from *Aspergillus fumigatus*. Energy 2020;190:116395. https://doi.org/10.1016/j.energy.2019.116395.

[9] Jugwanth Y, Sewsynker-Sukai Y, Gueguim Kana EB. Valorization of sugarcane bagasse for bioethanol production through simultaneous saccharification and fermentation: Optimization and kinetic studies. Fuel 2020;262:116552. https://doi.org/10.1016/j.fuel.2019.116552.

[10] Siriwong T, Laimeheriwa B, Aini UN, et al. Cold hydrolysis of cassava pulp and its use in simultaneous saccharification and fermentation (SSF) process for ethanol fermentation. J Biotechnol 2019;292:57–63. https://doi.org/10.1016/j.jbiotec.2019.01.003. PMid: 30690096.

[11] Lynd LR, Liang X, Biddy MJ, et al. Cellulosic ethanol: status and innovation. Curr Opin Biotechnol 2017;45:202–11. https://doi.org/10.1016/j.copbio.2017.03.008. PMid: 28528086.

[12] Su T, Zhao D, Khodadadi M, et al. Lignocellulosic biomass for bioethanol: Recent advances, technology trends, and barriers to industrial development. Curr Opin Green Sustain Chem 2020;24:56–60. https://doi.org/10.1016/j.cogsc.2020.04.005.

[13] Holou RAY, Stevens G. Juice, sugar, and bagasse response of sweet sorghum (*Sorghum bicolor* (L.) Moench cv. M81E) to N fertilization and soil type. GCB Bioenergy 2012;4(3):302–10. https://doi.org/10.1111/j.1757-1707.2011.01126.x.

[14] Rolz C, de León R, Mendizábal de Montenegro AL. Co-production of ethanol and biodiesel from sweet sorghum juice in two consecutive fermentation steps. Electron J Biotechnol 2019;41:13–21. https://doi.org/10.1016/j.ejbt.2019.05.002.

[15] Prasad S, Singh A, Jain N, et al. Ethanol production from sweet sorghum syrup for utilization as automotive fuel in India. Energy Fuel 2007;21(4):2415–20. https://doi.org/10.1021/ef060328z.

[16] Deesuth O, Laopaiboon P, Klanrit P, et al. Improvement of ethanol production from sweet sorghum juice under high gravity and very high gravity conditions: Effects of nutrient supplementation and aeration. Ind Crops Prod 2015;74:95–102. https://doi.org/10.1016/j.indcrop.2015.04.068.

[17] Camargos CV, Moraes VD, de Oliveira LM, et al. High gravity and very high gravity fermentation of sugarcane molasses by flocculating *Saccharomyces cerevisiae*: Experimental investigation and kinetic modeling. Appl Biochem Biotechnol 2021;193:807–21. https://doi.org/10.1007/s12010-020-03466-9. PMid: 33196971.

[18] Bai FW, Anderson WA, Moo-Young M. Ethanol fermentation technologies from sugar and starch feedstocks. Biotechnol Adv 2008;26(1):89–105. https://doi.org/10.1016/j.biotechadv.2007.09.002. PMid: 17964107.

[19] Laopaiboon L, Suporn S, Klanrit P, et al. Novel effective yeast strains and their performance in high gravity and very high gravity ethanol fermentations from sweet sorghum juice. Energies 2021;14(3):557. https://doi.org/10.3390/en14030557.

[20] Zhang X, Wang L, Li Q, et al. Omics analysis reveals mechanism underlying metabolic oscillation during continuous very-high-gravity ethanol fermentation by *Saccharomyces cerevisiae*. Biotechnol Bioeng 2021;118(8):2990–3001. https://doi.org/10.1002/bit.27809. PMid: 33934328.

[21] Larnaudie V, Rochón E, Ferrari MD, et al. Energy evaluation of fuel bioethanol production from sweet sorghum using very high gravity (VHG) conditions. Renew Energy 2016;88:280–7. https://doi.org/10.1016/j.renene.2015.11.041.

[22] Phutela UG, Kaur J. Process optimization for ethanol production from sweet sorghum juice using *Saccharomyces cerevisiae* strain NRRL Y-2034 by response surface methodology. Sugar Tech 2014;16:411–21. https://doi.org/10.1007/s12355-013-0283-0.

[23] Nuanpeng S, Thanonkeo S, Klanrit P, et al. Ethanol production from sweet sorghum by *Saccharomyces cerevisiae* DBKKUY-53 immobilized on alginate-loofah matrices. Braz J Microbiol 2018;49(Supp 1):140–50. https://doi.org/10.1016/j.bjm.2017.12.011. PMid: 29588196.

[24] Sriputorn B, Laopaiboon P, Phukoetphim N, et al. Enhancement of ethanol production efficiency in repeated-batch fermentation from sweet sorghum stem juice: Effect of initial sugar, nitrogen and aeration. Electron J Biotechnol 2020;46:55–64. https://doi.org/10.1016/j.ejbt.2020.06.001.

[25] Ariyajaroenwong P, Laopaiboon P, Salakkam A, et al. Kinetic models for batch and continuous ethanol fermentation from sweet sorghum juice by yeast immobilized on sweet sorghum stalks. J Taiwan Inst Chem Eng 2016;66:210–6. https://doi.org/10.1016/j.jtice.2016.06.023.

[26] Ariyajaroenwong P, Laopaiboon P, Laopaiboon L. Improvement of batch and continuous ethanol fermentations from sweet sorghum stem juice in a packed bed bioreactor by immobilized yeast cells under microaeration. Bioresour Technol Rep 2022;17:100908. https://doi.org/10.1016/j.biteb.2021.100908.

[27] Martínez-Jimenez FD, Pereira IO, Ribeiro MPA, et al. Integration of first- and second-generation ethanol production: Evaluation of a mathematical model to describe sucrose and xylose co-fermentation by recombinant *Saccharomyces cerevisiae*. Renew Energy 2022;192:326–39. https://doi.org/10.1016/j.renene.2022.04.094.

[28] Thangprompan P, Thanapimmetha A, Saisriyoot M, et al. Production of ethanol from sweet sorghum juice using VHG technology: A simulation case study. Appl Biochem Biotechnol 2013;171:294–314. https://doi.org/10.1007/s12010-013-0365-1. PMid: 23832188.

[29] Phukoetphim N, Salakkam A, Laopaiboon P, et al. Kinetic models for batch ethanol production from sweet sorghum juice under normal and high gravity fermentations: Logistic and modified Gompertz models. J Biotechnol 2017;243:69–75. https://doi.org/10.1016/j.jbiotec.2016.12.012. PMid: 27988216.

[30] Deesuth O, Laopaiboon P, Laopaiboon L. High ethanol production under optimal aeration conditions and yeast composition in a very high gravity fermentation from sweet sorghum juice by *Saccharomyces cerevisiae*. Ind Crops Prod 2016;92:263–70. https://doi.org/10.1016/j.indcrop.2016.07.042.

[31] Mecozzi M. Estimation of total carbohydrate amount in environmental samples by the phenol–sulphuric acid method assisted by multivariate calibration. Chemom Intell Lab Syst 2005;79(1–2):84–90. https://doi.org/10.1016/j.chemolab.2005.04.005.

[32] Moungprayoon A, Lunprom S, Reungsang A, et al. High cell density cultivation of *Paracoccus* sp. on sugarcane juice for poly(3-hydroxybutyrate) production. Front Bioeng Biotechnol 2022;10:878688. https://doi.org/10.3389/fbioe.2022.878688. PMid: 35646885.

[33] Tseng MMC, Wayman M. Kinetics of yeast growth: inhibition-threshold substrate concentrations. Can J Microbiol 1975;21(7):994–1003. https://doi.org/10.1139/m75-147. PMid: 1097079.

[34] Ghose TK, Tyagi RD. Rapid ethanol fermentation of cellulose hydrolysate. II. Product and substrate inhibition and optimization of fermentor design. Biotechnol Bioeng 1979;21(8):1401–20. https://doi.org/10.1002/bit.260210808.

[35] Keklik NM, Demirci A, Puri VM, et al. Modeling the inactivation of *Salmonella typhimurium*, *Listeria monocytogenes*, and *Salmonella enteritidis* on poultry products exposed to pulsed UV light. J Food Prot 2012;75(2):281–8. https://doi.org/10.4315/0362-028X.JFP-11-298. PMid: 22289588.

[36] Ross T. Indices for performance evaluation of predictive models in food microbiology. J Appl Bacteriol 1996;81(5):501–8. https://doi.org/10.1111/j.1365-2672.1996.tb03539.x. PMid: 8939028.

[37] Germec M, Cheng KC, Karhan M, et al. Application of mathematical models to ethanol fermentation in biofilm reactor with carob extract. Biomass Convers Biorefin 2020;10:237–52. https://doi.org/10.1007/s13399-019-00425-1.

[38] Zhao S. Enhanced ethanol production from stalk juice of sweet sorghum by response surface methodology. Afr J Biotechnol 2012;11(22):6117–22. https://doi.org/10.5897/AJB11.1701.

[39] Techaparin A, Thanonkeo P, Klanrit P. High-temperature ethanol production using thermotolerant yeast newly isolated from Greater Mekong Subregion. Braz J Microbiol 2017;48(3):461–75. https://doi.org/10.1016/j.bjm.2017.01.006. PMid: 28365094.

[40] Koch AL. The Monod model and its alternatives. In: Koch AL, Robinson JA, Milliken GA, editors. Mathematical Modeling in Microbial Ecology. Boston: Springer US; 1998. p. 62–93. https://doi.org/10.1007/978-1-4615-4078-6_4.

[41] Gonzalez R, Morales P, Tronchoni J, et al. New genes involved in osmotic stress tolerance in *Saccharomyces cerevisiae*. Front Microbiol 2016;7:1545. https://doi.org/10.3389/fmicb.2016.01545.

[42] Munna MS, Humayun S, Noor R. Influence of heat shock and osmotic stresses on the growth and viability of *Saccharomyces cerevisiae* SUBSC01. BMC Res Notes 2015;8:369. https://doi.org/10.1186/s13104-015-1355-x. PMid: 26298101.

[43] Laroche C, Beney L, Marechal P, et al. The effect of osmotic pressure on the membrane fluidity of *Saccharomyces cerevisiae* at different physiological temperatures. Appl Microbiol Biotechnol 2001;56:249–54. https://doi.org/10.1007/s002530000583. PMid: 11499939.

[44] Kargi F. Re-interpretation of the logistic equation for batch microbial growth in relation to Monod kinetics. Lett Appl Microbiol 2009;48(4):398–401. https://doi.org/10.1111/j.1472-765X.2008.02537.x.

[45] Zhang Q, Wu D, Lin Y, et al. Substrate and product inhibition on yeast performance in ethanol fermentation. Energy Fuels 2015;29(2):1019–27. https://doi.org/10.1021/ef502349v.

[46] Abdelghani GL. Continuous ethanol fermentation at very high gravity in the presence of *Saccharomyces cerevisiae*: A bifurcation analysis. J Sustain Bioenergy Syst 2018;8(4):116–26. https://doi.org/10.4236/jsbs.2018.84009.

[47] Doran MP. Reactor Engineering. In: Doran MP, editor. Bioprocess Engineering Principles. London: Academic Press; 1995. p. 333–91. https://doi.org/10.1016/B978-012220855-3/50013-4.

[48] Almquist J, Cvijovic M, Hatzimanikatis V, et al. Kinetic models in industrial biotechnology – Improving cell factory performance. Metab Eng 2014;24:38–60. https://doi.org/10.1016/j.ymben.2014.03.007. PMid: 24747045.

[49] Oliveira SC, De Castro HF, Visconti AES, et al. Continuous ethanol fermentation in a tower reactor with flocculating yeast recycle: scale-up effects on process performance, kinetic parameters and model predictions. Bioprocess Eng 1999;20:525–30. https://doi.org/10.1007/s004490050624.